OL | Organic Letters

pubs.acs.org/OrgLett

Letter

Axially Chiral Stable Radicals: Resolution and Characterization of Blatter Radical Atropisomers

Agnieszka Bodzioch,* Anna Pietrzak, and Piotr Kaszyński*

Cite This: *Org. Lett.* 2021, 23, 7508–7512

Read Online

ACCESS | Metrics & More | Article Recommendations | Supporting Information

ABSTRACT: Atropisomers of three Blatter radicals were obtained by the addition of 8-substituted 1-naphthyllithiums to 3-phenyl and 3-*t*-butylbenzo[*e*][1,2,4]triazine and separated by chiral high-performance liquid chromatography. Their absolute configurations were assigned by a comparison of experimental and time-dependent density functional theory calculated electronic circular dichroism spectra. The free energy of activation, $\Delta G^{\ddagger}_{298}$, and the half life of racemization, $t_{1/2}$, at 298 K were determined at ~25 kcal mol^{-1} and <130 h, respectively. Intramolecular $\pi-\pi$ interactions in radicals were evident from single-crystal X-ray diffraction, density functional theory, and electrochemical analyses.

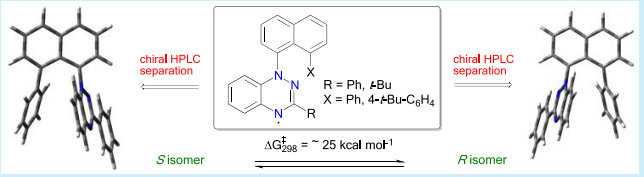

Electronic, electrochemical, and magnetic properties arising from the presence of an unpaired electron make stable organic radicals attractive and increasingly important structural elements of advanced functional materials for technological applications, such as molecular electronics,[1] energy storage,[2−4] and efficient organic light-emitting diodes.[5−8] A combination of the unpaired electron spin with the chiral molecular structure opens up new possibilities in the construction of molecules with unique magnetic and chirooptical features. Such derivatives are sought after for the investigation of spin-polarized electron transport[9] and chirality-induced spin selectivity[10−12] in the context of spintronic applications,[13−16] for studies of magneto-optical phenomena, such as magneto-chiral dichroism (MChD),[17] and for obtaining multifunctional solid materials and molecular magnets.[18−20] Other investigations demonstrated an efficient polarized emission,[21] electrical magnetochiral anisotropy,[22] and quantum teleportation[23] in some chiral radical derivatives.

Among the known stable chiral radicals,[24−33] there are only five examples **I**−**V** (Figure 1) of electrically neutral radicals with spin delocalized over chiral π frameworks.[28−32] Out of these,

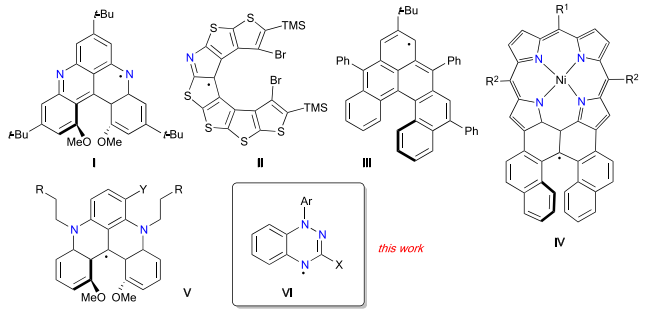

Figure 1. Chiral stable radicals with π-delocalized electron spin.

Scheme 1. Preparation of Radicals *rac*-1 from Benzo[*e*][1,2,4]triazines 2[a]

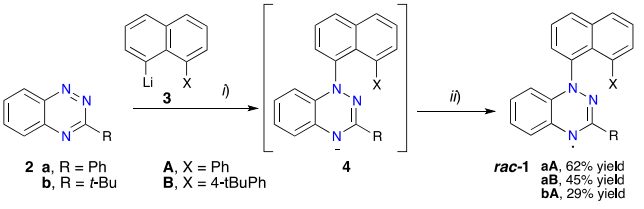

[a]Reagents and conditions: (i) naphthyllitium **3** (1.3 equiv), THF, −78 °C; (ii) H_2O, air. Yield of isolated radicals after chromatography.

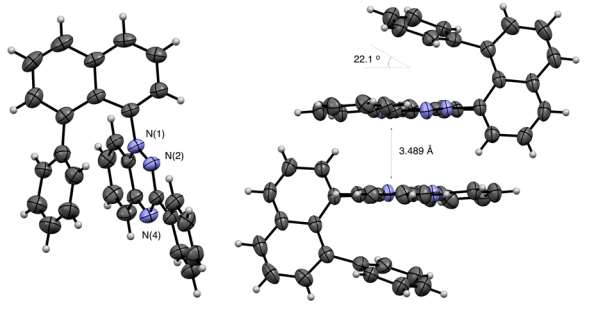

Figure 2. XRD structure of radical ***rac*-1aA** (left) and view of the enantiomeric pair in the unit cell (right). Thermal ellipsoids at 50% probability level. Pertinent dimensions: N(1)−C_{nath} 1.440(2) Å, C(3)−C_{Ph} 1.489(2) Å, C_{Naph}−C_{Ph} 1.492(2) Å; interplanar angles: Naphth/Ph 58.9°, Naphth/BT 67.5°, BT/Ph 7.6°.

Received: August 16, 2021
Published: September 17, 2021

https://doi.org/10.1021/acs.orglett.1c02733
Org. Lett. 2021, 23, 7508−7512

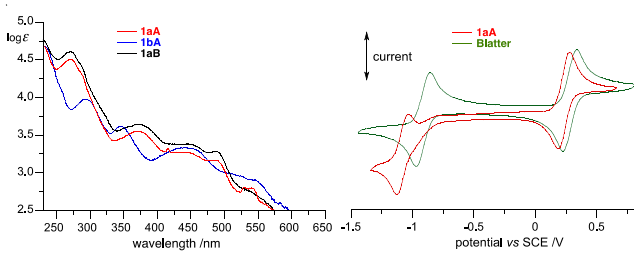

Figure 3. Left: UV−vis spectra for radicals **1** in CH_2Cl_2. Right: Cyclic voltammograms for the Blatter radical and **1aA** (0.5 mM) in CH_2Cl_2 ($[Bu_4N]^+PF_6^-$) (50 mM), ca. 20 °C, 50 mV s^{-1}, glassy carbon electrode.

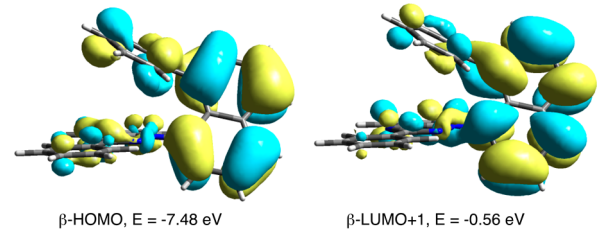

Figure 4. TD-DFT contours and energies of molecular orbitals relevant to the lowest energy excitation in **1aA**.

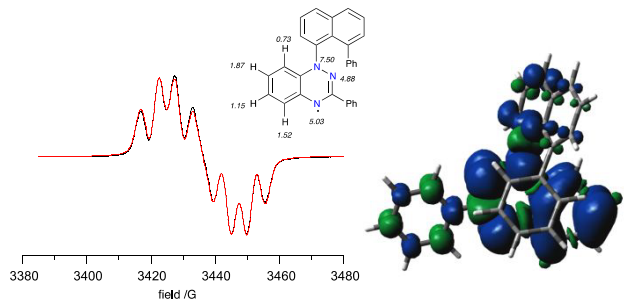

Figure 5. Left: Experimental (black) and simulated (red) EPR spectra for ***rac*-1aA** recorded in benzene. Inset shows an assignment of the resulting *hfcc*. Right: Total spin density in ***aR*-1aA**. Contour values are plotted at ±0.02 $(e/bohr^3)^{1/2}$.

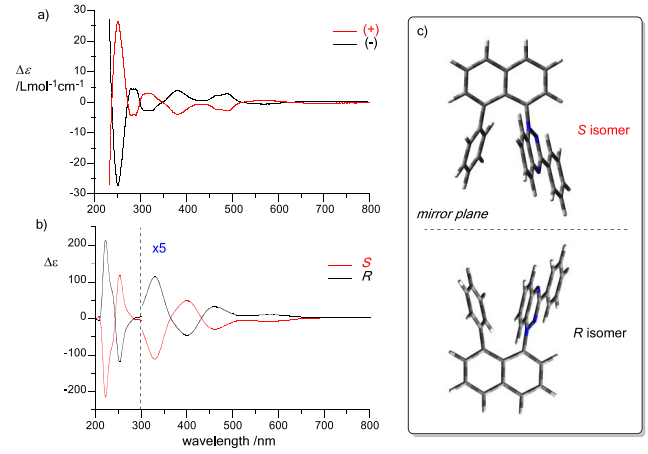

Figure 6. (a) Experimental ECD spectra of atropisomers of radical **1aA** in CH_2Cl_2. (b) TD-DFT calculated ECD spectra of **1aA** in CH_2Cl_2. (c) Configuration of S and R atropisomers of **1aA**. For details, see the SI.

only **I**,[28] **III**,[30] and **IV**[31] have been resolved into enantiomers and investigated in some detail.

The observed chemical reactivity, poor configurational stability, and synthetic difficulties are the main factors limiting the broader access to this class of unusual molecules. In this context, the exceptional stability, well developed chemistry,[34−37] and favorable electrochemical properties[38,39] make the 1,4-dihydrobenzo[*e*][1,2,4]triazin-4-yl (BT) core of radical **VI**[37,40,41] (Figure 1) an attractive candidate for a structural element of a broad class of chiral paramagnetic materials.

Herein we report on axially chiral derivatives of the Blatter radical (**VI**, Ar = X = Ph) obtained by the introduction of sterically hindered substituents at the N(1) and C(3) positions and chiral high-performance liquid chromatography (HPLC) separation of the resulting ***rac*-1** into atropisomeric pairs. The configurational stability of the enantiomers was assessed by kinetic methods, and the absolute configuration was assigned by a combination of chiroptical spectroscopy and time-dependent density functional theory (TD-DFT) calculations.

The racemic radicals ***rac*-1** were obtained by the azaphilic addition[42] of 8-substituted 1-naphthylithiums **3A** (X = Ph) and **3B** (X = 4-*t*-BuPh) to benzo[*e*][1,2,4]triazines **2a** (R = Ph) and **2b** (R = *t*-Bu, Scheme 1). The initially formed anion **4** was quenched with water, and the resulting *leuco* form was oxidized to ***rac*-1** by exposure to air. Pure radicals ***rac*-1** were isolated by column chromatography on a passivated SiO_2 support in yields diminishing from 62 to 29%. The observed trend apparently follows that in the steric congestion in series **1**.

The structure of racemic radical ***rac*-1aA** was confirmed with a single-crystal X-ray diffraction (XRD) analysis (Figure 2). The dimensions of the benzo[*e*][1,2,4]triazine (BT) heterocycle are typical for this ring system.[39,43,44] The C(3) phenyl group is nearly coplanar with the BT heterocycle forming the interplanar angle of 7.6°. Substitution of the naphthyl at the C(8) position resulted in a decrease in the torsion angle between the heterocycle and the naphthalene ring plane in comparison with the previously reported 1-(naphth-1-yl)-3-phenyl-1,4-dihydrobenzo[*e*][1,2,4]-triazin-4-yl[44] (67.5 vs 85.1°). The naphthalene ring and its C(8) phenyl substituent form a 58.9° dihedral angle that results in an approximately parallel orientation of the latter and the BT core with an interplanar

Table 1. Cyclic Voltammetry Data[a] and Estimated Energies of the FMOs for Radicals 1

radical	$E_{1/2}^{-1/0}$ (V)	$E_{1/2}^{0/+1}$ (V)	E_{cell} (V)[b]	E_{LUMO} (eV)[c]	E_{HOMO} (eV)[c]
Blatter[d]	−0.92	0.28	1.20	−3.81	−4.81
1aA	−1.08	0.23	1.31	−3.70	−4.79
1aB	−1.09	0.15	1.24	−3.66	−4.71
1bA	−1.13	0.21	1.34	−3.62	−4.77

[a]Conditions: $[nBu_4N]^+PF_6^-$ in CH_2Cl_2 (50 mM), ca. 20 °C, 50 mV s^{-1}, glassy carbon electrode. Potentials referenced against the Fc/Fc^+ couple (0.46 V vs SCE, ref 46). [b]$E_{cell} = E_{1/2}^{0/+1} - E_{1/2}^{-1/0}$. [c]Calculated from the onset of oxidation or reduction: $E_{HOMO/LUMO} = -(E_{(onset\ ox/red\ vs\ Fc+/Fc)} + 5.1)$; ref 47. [d]Ref 42.

https://doi.org/10.1021/acs.orglett.1c02733
Org. Lett. 2021, 23, 7508−7512

Table 2. Thermodynamic Data for Thermal Enantiomerization of Atropisomers 1 in 1,2-Dichloroethane[a]

radical	E_a (kcal mol^{-1})[b]	$\Delta H^{\ddagger}$ (kcal mol^{-1})[c]	$\Delta S^{\ddagger}$ (cal mol^{-1} K^{-1})[c]	$\Delta G^{\ddagger}_{298}$ (kcal mol^{-1})[c]	$t_{1/2(298)}$ (h)[d]
1aA	23.3 ± 0.3	22.6 ± 0.3	−6.8 ± 1.0	24.7 ± 0.3	20
1aB	24.4 ± 0.2	23.8 ± 0.2	−5.6 ± 0.7	25.4 ± 0.2	70
1bA	22.5 ± 0.5	21.8 ± 0.5	−13.3 ± 1.6	25.8 ± 0.5	130

[a]For the racemization process, the entropy is larger by +1.4 cal mol^{-1} K^{-1}, and the free energy is smaller by 0.4 kcal mol^{-1}. [b]From the Arrhenius analysis. [c]From the Eyring analysis. [d]Estimated order of magnitude for the racemization half life calculated using $k_{rac} = 2 \times k_{en}$ obtained from the extrapolation of kinetic data. For details, see the SI.

angle of 22.1°. The shortest nonbonding distances are found between the N(1) and N(2) atoms of the triazine and the C atoms of the cofacial benzene ring (2.916(1) and 3.077(7) Å, respectively). The molecules form discrete dimeric pairs of enantiomers related by a symmetry center and an interplanar separation of 3.489 Å (Figure 2).

To assess the effect of the intramolecular $\pi-\pi$ interactions on the electronic properties, we analyzed radicals ***rac*-1** by spectroscopic (UV−vis and electron paramagnetic resonance (EPR)) and electrochemical methods.

All radicals **1** exhibit a broad, low-intensity absorption in the visible range up to 600 nm similar to that observed in the parent Blatter radical[42,45] and quasi-reversible redox behavior (Figure 3). A comparison of the data in Table 1 revealed a cathodic shift of the oxidation potentials by up to 0.13 V and a more pronounced shift of the reduction potential by up to 0.21 V in radicals **1** relative to the parent Blatter radical[38,42] (**VI**, X = Ar = Ph). This indicates that the frontier molecular orbital (FMO) energies become more positive, and the electrochemical window in **1** is expanded by up to 0.14 V relative to those in the parent Blatter (Table 1).[42]

The electrochemical data are consistent with the results of the TD-DFT calculations in the CH_2Cl_2 dielectric medium. The results show that the intramolecular $\pi-\pi$ interactions between the cofacial Ph and BT rings in **1a** destabilize the FMOs, both localized on the BT core. Thus the α-HOMO is higher by up to 0.038 eV and the β-LUMO is higher by ∼0.066 eV relative to those in the Blatter, which leads to the net expansion of the HOMO−LUMO gap. The TD-DFT results also show that the cofacial $\pi-\pi$ interactions change the nature of the low energy excitations in **1**. Thus the lowest energy excitation calculated for **1aA** at 530.1 nm is mainly due to transitions involving the naphthyl fragment with some contributions from the BT and cofacial benzene rings (Figure 4), whereas the excitation at 425 nm originates from the transitions within the benzo[*e*][1,2,4]-triazinyl with some contribution from the cofacial benzene ring.

Radicals **1** exhibit typical EPR spectra consisting of seven principal lines (*e.g.*, ***rac*-1aA** in Figure 5) with the a_{N1}, a_{N2}, and a_{N4} *hfcc* values similar to those in the prototypical Blatter radical, about 7.5, 4.9, and 5.0 G, respectively.

Racemic mixtures of benzo[*e*][1,2,4]triazinyls ***rac*-1** were resolved into enantiomers using a semipreparative HPLC method and a Chiralcel OD-H stationary phase, which was found to be the most effective. For instance, enantiomers of **1aA** are separated by over 2 min with retention times of 14.5 and 16.8 min.[48]

Optical rotation analysis established that the isomer eluted in the first HPLC fraction is dextrorotatory (+) for all three radicals **1**. Electronic circular dichroism (ECD) measurements in CH_2Cl_2 solutions demonstrated that (+) enantiomers of the C(3)−Ph-substituted radicals, (+)-**1aA** and (+)-**1aB**, exhibit a positive Cotton effect (CE) around 250 and 320 nm and a negative CE at ∼220 (maximum below the transparency window) and above 350 nm (Figure 6). In contrast, the analogous C(3)−*t*-Bu derivative, (+)-**1bA**, exhibits an opposite trend in the Cotton effect.[48] The leverotatory enantiomers (−)-**1** gave ECD spectra, which are mirror images of those for the (+)-**1** enantiomers, as shown for **1aA** in Figure 6. The assignment of absolute configuration to individual enantiomers **1** was accomplished by a comparison of the experimental ECD spectra with those calculated with TD-DFT methods (UCAM-B3LYP/Def2SVP//UB3LYP/Def2SVP level of theory).[48] Thus the analysis suggests that all (+)-**1** isomers have the S configuration, whereas the (−)-**1** analogues have the R configuration.

The configurational stability of radicals **1** was investigated as a time-dependent decay of enantiomeric excess (*ee*) in 1,2-dichloroethane (DCE) solutions, and the thermodynamic parameters for the enantiomer interconversion process were determined from the Eyring analysis of the first-order kinetic data.[48] The data in Table 2 show that the activation enthalpy, $\Delta H^{\ddagger}$, for the enantiomerization process[49] is ∼23 kcal mol^{-1} for the C(3)−Ph derivatives **1a** and up to 2 kcal mol^{-1} lower for the C(3)−*t*-Bu radical **1bA**. Combined with the negative entropy of activation, $\Delta S^{\ddagger}$, the resulting free energy of activation, $\Delta G^{\ddagger}_{298}$, for the enantiomerization is ∼25 kcal mol^{-1} for all three radicals. Interestingly, the largest entropy of activation is measured for **1bA** (−13.3 ± 1.6 cal mol^{-1} K^{-1}), which gives the highest value in the series of free energy of activation, $\Delta G^{\ddagger}_{298}$, (25.8 ± 0.5 kcal mol^{-1}) despite the lowest $\Delta H^{\ddagger}$. The order of $\Delta G^{\ddagger}_{298}$ values in the series is paralleled by the order of the half life of the racemization process at standard temperature, $t_{1/2(298)}$, calculated from the rate constant of racemization ($k_{rac} = 2 \times k_{en}$)[49] extrapolated to T = 298 K. Although the uncertainty for such an estimate is high, the obtained $t_{1/2(298)}$ values demonstrate the highest configurational stability of the C(3)−*t*-Bu derivative **1bA** with the estimated decay of the enantiomeric excess *ee* to 50% after ∼130 h (Table 2). Overall, the data in Table 2 indicate that expanding the size of the naphthalene ring C(8) substituent (from Ph in **1aA** to C_6H_4-4-*t*Bu in **1aB**) increases the enthalpic barrier of the enantiomer interconversion, whereas changing the C(3)−Ph in **1aA** to C(3)-*t*-Bu in **1bA** stabilizes the atropisomers entropically.

A similar kinetic analysis of enantiopure **1aA** in cyclohexane solutions gave very different results: A much larger activation enthalpy ($\Delta H^{\ddagger}$ = 38.8 ± 1.5 kcal mol^{-1}) and a significantly positive activation entropy ($\Delta S^{\ddagger}$ = 42.5 ± 4.5 cal mol^{-1} K^{-1}) were obtained, although the resulting free energy of activation, $\Delta G^{\ddagger}_{298}$, remains comparable to that obtained from the DCE solutions.[48] The observed significantly positive $\Delta S^{\ddagger}$ value indicates a less ordered transition state than the ground state and suggests the presence of aggregates, which must break apart prior to the interconversion to the opposite enantiomer.

In summary, we have demonstrated the preparation and chiral resolution of the first axially chiral derivatives of the Blatter radical. The kinetic stability of the enantiomeric radicals **1**,

https://doi.org/10.1021/acs.orglett.1c02733
Org. Lett. 2021, 23, 7508−7512

$\Delta G^{\ddagger}_{298} \approx 25$ kcal mol^{-1}, appears to be sufficient for their further studies and for their incorporation into other molecular systems using functional group transformations already developed for the benzo[*e*][1,2,4]triazin-4-yl derivatives.

The presented synthetic method opens up access to a potentially rich class of easily accessible robust chiral paramagnetic materials and building blocks of type **VI**, whose properties such as the configurational stability, transannular electronic interactions, and redox and photophysical behavior can be fine-tuned by a judicious choice of substituents.

■ ASSOCIATED CONTENT

Supporting Information

The Supporting Information is available free of charge at https://pubs.acs.org/doi/10.1021/acs.orglett.1c02733.

Preparative and analytical details, NMR and FTIR spectra, XRD data, UV−vis, EPR, E-chem, kinetic data, and computational details (PDF)

FAIR data, including the primary NMR FID files, for compounds **2b**, **3A**, **3B**, and **5** (ZIP)

Accession Codes

CCDC 2087259 contains the supplementary crystallographic data for this paper. These data can be obtained free of charge via www.ccdc.cam.ac.uk/data_request/cif, or by emailing data_request@ccdc.cam.ac.uk, or by contacting The Cambridge Crystallographic Data Centre, 12 Union Road, Cambridge CB2 1EZ, UK; fax: +44 1223 336033.

■ AUTHOR INFORMATION

Corresponding Authors

Piotr Kaszyński − *Centre of Molecular and Macromolecular Studies, Polish Academy of Sciences, 90-363 Łódź, Poland; Faculty of Chemistry, University of Łódź, 91-403 Łódź, Poland; Department of Chemistry, Middle Tennessee State University, Murfreesboro, Tennessee 37132, United States;* orcid.org/0000-0002-2325-8560; Email: PiotrK@cbmm.lodz.pl

Agnieszka Bodzioch − *Centre of Molecular and Macromolecular Studies, Polish Academy of Sciences, 90-363 Łódź, Poland;* orcid.org/0000-0002-4501-4639; Email: agabodz@cbmm.lodz.pl

Author

Anna Pietrzak − *Faculty of Chemistry, Łódź University of Technology, 90-024 Łódź, Poland;* orcid.org/0000-0003-3415-8650

Complete contact information is available at: https://pubs.acs.org/10.1021/acs.orglett.1c02733

Notes

The authors declare no competing financial interest.

■ ACKNOWLEDGMENTS

This work was supported by the Foundation for Polish Science (TEAM/2016-3/24) and National Science Centre (2020/38/A/ST4/00597 and 2019/03/X/ST4/01147) grants. We thank Prof. Piotr Chmielewski (Wrocław University) for assistance with ECD measurements.

■ REFERENCES

(1) Ji, L.; Shi, J.; Wei, J.; Yu, T.; Huang, W. Air-stable organic radicals: New-generation materials for flexible electronics? *Adv. Mater.* **2020**, *32*, 1908015.

(2) Friebe, C.; Schubert, U. S. High-Power-Density Organic Radical Batteries. In *Electrochemical Energy Storage: Next Generation Battery Concepts*; Eichel, R.-A., Ed.; Springer: Cham, Switzerland, 2019; pp 65−99.

(3) Wilcox, D. A.; Agarkar, V.; Mukherjee, S.; Boudouris, B. W. Stable radical materials for energy applications. *Annu. Rev. Chem. Biomol. Eng.* **2018**, *9*, 83−103.

(4) Aqil, A.; Vlad, A.; Piedboeuf, M.-L.; Aqil, M.; Job, N.; Melinte, S.; Detrembleur, C.; Jérôme, C. A new design of organic radical batteries (ORBs): carbon nanotube buckypaper electrode functionalized by electrografting. *Chem. Commun.* **2015**, *51*, 9301−9304.

(5) Hudson, J. M.; Hele, T. J. H.; Evans, E. W. Efficient light-emitting diodes from organic radicals with doublet emission. *J. Appl. Phys.* **2021**, *129*, 180901.

(6) Cui, Z.; Abdurahman, A.; Ai, X.; Li, F. Stable luminescent radicals and radical-based LEDs with doublet emission. *CCS Chem.* **2020**, *2*, 1129−1145.

(7) Peng, Q.; Obolda, A.; Zhang, M.; Li, F. Organic light-emitting diodes using a neutral π radical as emitter: The emission from a doublet. *Angew. Chem., Int. Ed.* **2015**, *54*, 7091−7095.

(8) Ai, X.; Evans, E. W.; Dong, S.; Gillett, A. J.; Guo, H.; Chen, Y.; Hele, T. J. H.; Friend, R. H.; Li, F. Efficient radical-based light-emitting diodes with doublet emission. *Nature* **2018**, *563*, 536−540.

(9) Naaman, R.; Waldeck, D. H. Spintronics and chirality: Spin selectivity in electron transport through chiral molecules. *Annu. Rev. Phys. Chem.* **2015**, *66*, 263−281.

(10) Geyer, M.; Gutierrez, R.; Mujica, V.; Cuniberti, G. Chirality-induced spin selectivity in a coarse-grained tight-binding model for helicene. *J. Phys. Chem. C* **2019**, *123*, 27230−27241.

(11) Göhler, B.; Hamelbeck, V.; Markus, T. Z.; Kettner, M.; Hanne, G. F.; Vager, Z.; Naaman, R.; Zacharias, H. Spin selectivity in electron transmission through self-assembled monolayers of double-stranded DNA. *Science* **2011**, *331*, 894−897.

(12) Kiran, V.; Mathew, S. P.; Cohen, S. R.; Hernández-Delgado, I.; Lacour, J.; Naaman, R. Helicenes—A new class of organic spin filter. *Adv. Mater.* **2016**, *28*, 1957−1962.

(13) de Jong, M. P. Recent progress in organic spintronics. *Open Phys.* **2016**, *14*, 337−353.

(14) Sanvito, S. Molecular spintronics. *Chem. Soc. Rev.* **2011**, *40*, 3336−3355.

(15) Mas-Torrent, M.; Crivillers, N.; Mugnaini, V.; Ratera, I.; Rovira, C.; Veciana, J. Organic radicals on surfaces: Towards molecular spintronics. *J. Mater. Chem.* **2009**, *19*, 1691−1695.

(16) Casu, M. B. Nanoscale studies of organic radicals: Surface, interface, and spinterface. *Acc. Chem. Res.* **2018**, *51*, 753−760.

(17) Rikken, G. L. J. A.; Raupach, E. Observation of magneto-chiral dichroism. *Nature* **1997**, *390*, 493−494.

(18) Train, C.; Gruselle, M.; Verdaguer, M. The fruitful introduction of chirality and control of absolute configurations in molecular magnets. *Chem. Soc. Rev.* **2011**, *40*, 3297−3312.

(19) Minguet, M.; Luneau, D.; Lhotel, E.; Villar, V.; Paulsen, C.; Amabilino, D. B.; Veciana, J. An enantiopure molecular ferromagnet. *Angew. Chem., Int. Ed.* **2002**, *41*, 586−589.

(20) Inoue, K.; Ohkoshi, S.-i.; Imai, H. Chiral Molecule-Based Magnets In *Magnetism: Molecules to Materials V*; Miller, J. S., Drillon, M., Eds.; Wiley-VCH: Weinheim, Germany, 2005; pp 41−70.

(21) Mayorga Burrezo, P.; Jimenez, V. G.; Blasi, D.; Ratera, I.; Campana, A. G.; Veciana, J. Organic free radicals as circularly polarized luminescence emitters. *Angew. Chem., Int. Ed.* **2019**, *58*, 16282−16288.

(22) Pop, F.; Auban-Senzier, P.; Canadell, E.; Rikken, G. L. J. A.; Avarvari, N. Electrical magnetochiral anisotropy in a bulk chiral molecular conductor. *Nat. Commun.* **2014**, *5*, 3757.

(23) Rugg, B. K.; Krzyaniak, M. D.; Phelan, B. T.; Ratner, M. A.; Young, R. M.; Wasielewski, M. R. Photodriven quantum teleportation

of an electron spin state in a covalent donor-acceptor-radical system. *Nat. Chem.* **2019**, *11*, 981−986.
(24) Zak, J. K.; Miyasaka, M.; Rajca, S.; Lapkowski, M.; Rajca, A. Radical cation of helical, cross-conjugated β-oligothiophene. *J. Am. Chem. Soc.* **2010**, *132*, 3246−3247.
(25) Gliemann, B. D.; Petrovic, A. G.; Zolnhofer, E. M.; Dral, P. D.; Hampel, F.; Breitenbruch, G.; Schulze, P.; Raghavan, V.; Meyer, K.; Polavarapu, P. L.; Berova, N.; Kivala, M. Configurationally stable chiral dithia-bridged hetero[4]helicene radical cation: Electronic structure and absolute configuration. *Chem. - Asian J.* **2017**, *12*, 31−35.
(26) Shu, C.; Zhang, H.; Olankitwanit, A.; Rajca, S.; Rajca, A. High-spin diradical dication of chiral π-conjugated double helical molecule. *J. Am. Chem. Soc.* **2019**, *141*, 17287−17294.
(27) Kasemthaveechok, S.; Abella, L.; Jean, M.; Cordier, M.; Roisnel, T.; Vanthuyne, N.; Guizouarn, T.; Cador, O.; Autschbach, J.; Crassous, J.; Favereau, L. Axially and helically chiral cationic radical bicarbazoles: SOMO−HOMO level inversion and chirality impact on the stability of mono- and diradical cations. *J. Am. Chem. Soc.* **2020**, *142*, 20409−20418.
(28) Ueda, A.; Wasa, H.; Suzuki, S.; Okada, K.; Sato, K.; Takui, T.; Morita, Y. Chiral stable phenalenyl radical: Synthesis, electronic-spin structure, and optical properties of [4]helicene-structured diazaphenalenyl. *Angew. Chem., Int. Ed.* **2012**, *51*, 6691−6695.
(29) Wang, Y.; Zhang, H.; Pink, M.; Olankitwanit, A.; Rajca, S.; Rajca, A. Radical cation and neutral radical of aza-thia[7]helicene with SOMO−HOMO energy level inversion. *J. Am. Chem. Soc.* **2016**, *138*, 7298−7304.
(30) Ravat, P.; Ribar, P.; Rickhaus, M.; Haussinger, D.; Neuburger, M.; Juricek, M. Spin-delocalization in a helical open-shell hydrocarbon. *J. Org. Chem.* **2016**, *81*, 12303−12317.
(31) Kato, K.; Furukawa, K.; Mori, T.; Osuka, A. Porphyrin-based air-stable helical radicals. *Chem. - Eur. J.* **2018**, *24*, 572−575.
(32) Shaikh, A. C.; Moutet, J.; Veleta, J. M.; Hossain, M. M.; Bloch, J.; Astashkin, A. V.; Gianetti, T. A. Persistent, highly localized, and tunable [4]helicene radicals. *Chem. Sci.* **2020**, *11*, 11060−11067.
(33) Tani, F.; Narita, M.; Murafuji, T. Helicene radicals: Molecules bearing a combination of helical chirality and unpaired electron spin. *ChemPlusChem* **2020**, *85*, 2093−2104.
(34) Constantinides, C. P.; Koutentis, P. A.; Loizou, G. Synthesis of 7-aryl/heteraryl-1,3-diphenyl-1,2,4-benzotriazinyls via palladium catalyzed Stille and Suzuki-Miyaura reactions. *Org. Biomol. Chem.* **2011**, *9*, 3122−3125.
(35) Bodzioch, A.; Zheng, M.; Kaszynski, P.; Utecht, G. Functional group transformations in derivatives of 1,4-dihydrobenzo[1,2,4]-triazinyl radical. *J. Org. Chem.* **2014**, *79*, 7294−7310.
(36) Berezin, A. A.; Constantinides, C. P.; Mirallai, S. I.; Manoli, M.; Cao, L. L.; Rawson, J. M.; Koutentis, P. A. Synthesis and properties of imidazolo-fused benzotriazinyl radicals. *Org. Biomol. Chem.* **2013**, *11*, 6780−6795.
(37) Rogers, F. J. M.; Norcott, P. L.; Coote, M. L. Recent advances in the chemistry of benzo[e][1,2,4]triazinyl radicals. *Org. Biomol. Chem.* **2020**, *18*, 8255−8277.
(38) Berezin, A. A.; Zissimou, G.; Constantinides, C. P.; Beldjoudi, Y.; Rawson, J. M.; Koutentis, P. A. Route to benzo- and pyrido-fused 1,2,4-triazinyl radicals via N′-(het)aryl-N′-[2-nitro(het)aryl]hydrazides. *J. Org. Chem.* **2014**, *79*, 314−327.
(39) Savva, A. C.; Mirallai, S. I.; Zissimou, G. A.; Berezin, A. A.; Demetriades, M.; Kourtellaris, A.; Constantinides, C. P.; Nicolaides, C.; Trypiniotis, T.; Koutentis, P. A. Preparation of Blatter radicals via aza-Wittig chemistry: The reaction of N-aryliminophosphoranes with 1-(het)aroyl-2-aryldiazenes. *J. Org. Chem.* **2017**, *82*, 7564−7575.
(40) Ji, Y.; Long, L.; Zheng, Y. Recent advances of stable Blatter radicals: synthesis, properties and applications. *Mater. Chem. Front.* **2020**, *4*, 3433−3443.
(41) Constantinides, C. P.; Koutentis, P. K.; Krassos, H.; Rawson, J. M.; Tasiopoulos, A. J. Characterization and magnetic properties of a "super stable" radical 1,3-diphenyl-7-trifluoromethyl-1,4-dihydro-1,2,4-benzotriazin-4-yl. *J. Org. Chem.* **2011**, *76*, 2798−2806.
(42) Constantinides, C. P.; Obijalska, E.; Kaszyński, P. Access to 1,4-dihydrobenzo[e][1,2,4]triazin-4-yl derivatives. *Org. Lett.* **2016**, *18*, 916−919.
(43) Constantinides, C. P.; Koutentis, P. A.; Rawson, J. M. Ferromagnetic interactions in a 1D alternating linear chain of π-stacked 1,3-diphenyl-7-(thien-2-yl)-1,4-dihydro-1,2,4-benzotriazin-4-yl radicals. *Chem. - Eur. J.* **2012**, *18*, 7109−7116.
(44) Gardias, A.; Kaszyński, P.; Obijalska, E.; Trzybiński, D.; Domagała, S.; Woźniak, K.; Szczytko, J. Magnetostructural investigation of orthogonal 1-aryl-3-phenyl-1,4-dihydrobenzo[e][1,2,4]-triazin-4-yl derivatives. *Chem. - Eur. J.* **2018**, *24*, 1317−1329.
(45) Karecla, G.; Papagiorgis, P.; Panagi, N.; Zissimou, G. A.; Constantinides, C. P.; Koutentis, P. A.; Itskos, G.; Hayes, S. C. Emission from the stable Blatter radical. *New J. Chem.* **2017**, *41*, 8604−8613.
(46) Connelly, N. G.; Geiger, W. E. Chemical redox agents for organometallic chemistry. *Chem. Rev.* **1996**, *96*, 877−910.
(47) Cardona, C. M.; Li, W.; Kaifer, A. E.; Stockdale, D.; Bazan, G. C. Electrochemical considerations for determining absolute frontier orbital energy levels of conjugated polymers for solar cell applications. *Adv. Mater.* **2011**, *23*, 2367−2371.
(48) For details, see the SI.
(49) Reist, M.; Testa, B.; Carrupt, P.-A.; Jung, M.; Schurig, V. Racemization, enantiomerization, diastereomerization, and epimerization: Their meaning and pharmacological significance. *Chirality* **1995**, *7*, 396−400.

https://doi.org/10.1021/acs.orglett.1c02733
Org. Lett. 2021, 23, 7508−7512